Thermotropic liquid crystals from biomacromolecules

Kai Liu[a], Dong Chen[b], Alessio Marcozzi[a], Lifei Zheng[a], Juanjuan Su[c], Diego Pesce[a], Wojciech Zajaczkowski[d], Anke Kolbe[a], Wojciech Pisula[d], Klaus Müllen[d], Noel A. Clark[b,1], and Andreas Herrmann[a,1]

[a]Department of Polymer Chemistry, Zernike Institute for Advanced Materials and [c]Department of Molecular Dynamics, Groningen Biomolecular Sciences and Biotechnology Institute and Zernike Institute for Advanced Materials, University of Groningen, 9747 AG Groningen, The Netherlands; [b]Department of Physics and Liquid Crystal Materials Research Center, University of Colorado, Boulder, CO 80309-0390; and [d]Max Planck Institute for Polymer Research, 55128 Mainz, Germany

Contributed by Noel A. Clark, November 7, 2014 (sent for review August 26, 2014)

Complexation of biomacromolecules (e.g., nucleic acids, proteins, or viruses) with surfactants containing flexible alkyl tails, followed by dehydration, is shown to be a simple generic method for the production of thermotropic liquid crystals. The anhydrous smectic phases that result exhibit biomacromolecular sublayers intercalated between aliphatic hydrocarbon sublayers at or near room temperature. Both this and low transition temperatures to other phases enable the study and application of thermotropic liquid crystal phase behavior without thermal degradation of the biomolecular components.

biomaterial | liquid crystal | smectic | lipid | surfactant

Liquid crystals (LCs) play an important role in biology because their essential characteristic, the combination of order and mobility, is a basic requirement for self-organization and structure formation in living systems (1–3). Thus, it is not surprising that the study of LCs emerged as a scientific discipline in part from biology and from the study of myelin figures, lipids, and cell membranes (4). These and the LC phases formed from many other biomolecules, including nucleic acids (5, 6), proteins (7, 8), and viruses (9, 10), are classified as lyotropic, the general term applied to LC structures formed in water and stabilized by the distinctly biological theme of amphiphilic partitioning of hydrophilic and hydrophobic molecular components into separate domains. However, the principal thrust and achievement of the study of LCs has been in the science and application of thermotropic materials, structures, and phases in which molecules that are only weakly amphiphilic exhibit LC ordering by virtue of their steric molecular shape, flexibility, and/or weak intermolecular interactions [e.g., van der Waals and dipolar forces (11)]. These characteristics enable thermotropic LCs (TLCs) to adopt a wide variety of exotic phases and to exhibit dramatic and useful responses to external forces, including, for example, the electro-optic effects that have led to LC displays and the portable computing revolution. This general distinction between lyotropic LCs and TLCs suggests there may be interesting possibilities in the development of biomolecular or bioinspired LC systems in which the importance of amphiphilicity is reduced and the LC phases obtained are more thermotropic in nature. Such biological TLC materials are very appealing for several reasons. Most biomacromolecules were extensively characterized in aqueous environments, but in TLC phases, their solvent-free properties and functions could be investigated in a state in which no or only traces of water are present. Water exhibits a high dielectric constant and has the ability to form hydrogen bonds, greatly influencing the structure and functions of biomacromolecules or compromising electronic properties such as charge transport (12–15). Indeed, anhydrous TLC systems containing glycolipids (16–19), ferritin (20), and polylysine have been reported (21–23). However, a general approach to fabricating TLCs based on nucleic acids, polypeptides, proteins, and protein assemblies of large molecular weights such as virus particles remains elusive.

Here we propose that the combination of biomaterials with suitably chosen surfactants, followed by dehydration, can be effectively applied as a simple generic scheme for producing biomacromolecular-based TLCs. We demonstrate that biological TLCs can be made from a remarkable range of biomolecules and bio-inspired molecules, including nucleic acids, polypeptides, fusion proteins, and viruses. TLC materials typically combine rigid or semirigid anisometric units, which introduce orientational anisotropy, with flexible alkyl chains, which suppress crystallization (24). In the present experiments, negatively charged biomolecules and bio-inspired molecules act as rigid parts, and cationic surfactants make up the flexible units to produce TLC phases with remarkably low LC-isotropic clearing temperatures, which is another TLC signature. Electrostatic interactions couple these rigid and flexible components into hybrid assemblies, which then order into lamellar phases of alternating rigid and flexible layers (Fig. 1) stabilized by the tendency in TLCs for rigid and flexible to spatially segregate (25).

Results and Discussion

TLCs Based on Nucleic Acids. Inspired by previous work dealing with polyelectrolyte-lipid complexes (2, 26–31), for the preparation of nucleic acid TLCs, an oligonucleotide [22mer single-stranded DNA (ssDNA)] and the cationic surfactant dimethyldioctylammonium bromide (DOAB) were complexed in a simple procedure, including a final lyophilization step (*SI Appendix, Section B*). The solvent-free DNA–DOAB complex was birefringent (*SI Appendix*, Fig. S2) and viscous and did not solidify at room temperature. Thermogravimetric analysis of the DNA–surfactant melts revealed a water content of less than 3% (wt), confirming that only traces of water are present in the bulk material and that they are thermally stable up to 200 °C (*SI Appendix*, Fig. S3). The phase sequence was then investigated by polarized optical microscopy (POM). The typical focal-conic textures characteristic for smectic order (32) were observed on cooling from isotropic to the mesophase (Fig. 2*A*). Differential scanning calorimetry revealed two discrete

Significance

Liquid crystals (LCs) found in biology are usually dispersed in a solvent, typically water, and are therefore classified as lyotropic. However, from a technological perspective, thermotropic LCs (TLCs), typically based on small rod- or disc-shaped organic molecules, have been of much greater importance. In this contribution, we show that thermotropic liquid crystal phases and materials can also be made from biomolecules, demonstrating a simple generic method to form thermotropic phases from biosystems ranging from nucleic acids and proteins to even whole viruses, spanning a size from only a few nanometers to 1 μm.

Author contributions: K.L., D.C., K.M., N.A.C., and A.H. designed research; K.L., D.C., A.M., L.Z., J.S., D.P., W.Z., A.K., and W.P. performed research; K.L., A.M., L.Z., D.P., and A.K. contributed new reagents/analytic tools; K.L., D.C., L.Z., J.S., W.Z., A.K., W.P., K.M., N.A.C., and A.H. analyzed data; and K.L., D.C., K.M., N.A.C., and A.H. wrote the paper.

The authors declare no conflict of interest.

[1]To whom correspondence may be addressed. Email: noel.clark@colorado.edu or a.herrmann@rug.nl.

This article contains supporting information online at www.pnas.org/lookup/suppl/doi:10.1073/pnas.1421257111/-/DCSupplemental.

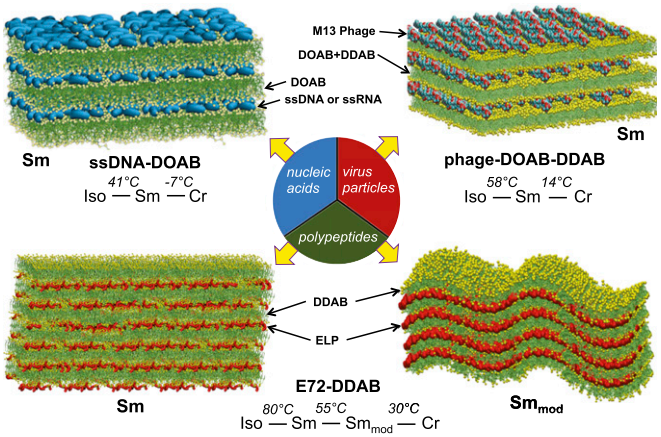

Fig. 1. Proposed structures of TLCs formed by the biological building blocks complexed with surfactants, showing sketches of various lamellar phases and the corresponding phase transition temperatures (°C). The lamellar bilayer structures are made of, alternately, a sublayer of the biomacromolecules and an interdigitated sublayer of the surfactants, where the negatively charged parts of the biomolecules (e.g., phosphate groups of ssDNA and ssRNA, glutamate residues of supercharged ELPs, and N-terminal glutamate and aspartate residues of pVIII protein in phages) electrostatically interact with the cationic head groups of the surfactants. For the ssDNA–DOAB and ssRNA–DOAB smectic TLCs, the oligonucleotides are randomly orientated in the DNA (RNA) sublayers. For the ELP–DDAB complexes, in addition to the bilayer smectic phase, a modulated smectic (Sm_{mod}) phase is observed at lower temperature. For the phage–DOAB–DDAB lamellar structures, rodlike virus particles are embedded in a sublayer between interdigitated surfactants with additional in-plane orientational order.

endothermic peaks at −7 and 41 °C, corresponding to crystalline–LC and LC–isotropic transitions, respectively (*SI Appendix*, Fig. S4). This finding suggests the formation of a TLC resulting from electrostatic complexation between the phosphate backbone of the oligonucleotide and the cationic head groups of DOAB because pristine DOAB is isotropic at the same temperature range.

The sharp reflection peak $q_1 = 0.314$ Å^{-1} and its harmonics $q_2 = 0.629$ Å^{-1} at small-angle X-ray scattering (SAXS) (Fig. 3*A* and *SI Appendix*, Fig. S5) indicate long-range ordered smectic layers of the DN–DOAB complexes with a periodicity of 20.0 Å ($d = 2\pi/q_1$). Considering the dimensions of the ssDNA and the DOAB, the layer spacing of 20.0 Å suggests the lamellar structure is composed of a ssDNA sublayer ∼10 Å thick (33) that electrostatically interacts with an interdigitated DOAB sublayer of ∼10 Å, as modeled in Fig. 1 and shown in the inset of Fig. 3*A*. In the wide-angle X-ray scattering (WAXS) experiment (Fig. 3*B*), the broad peak at $q = 1.45$ Å^{-1} corresponds to repeat distance of 4.3 Å, which is attributed to the intralayer packing of the alkyl chains of the surfactant (20). Regarding the X-ray results, no peak from the DNA intralayer packing was observed, which suggests that the oligonucleotide chains of ssDNA are randomly packed within the sublayer, without any positional or orientational order (34). The lamellar structure of the DNA–DOAB complex was directly visualized by freeze-fracture transmission electron microscopy (FF-TEM). As shown in Fig. 4*A*, stacks of flat and smooth layers with occasional distinct layer steps (yellow arrow) indicate a long-range order of the DNA–DOAB smectic mesophase. No specific or identifiable features were observed at the fracturing surface, even at high magnification (Fig. 4*B*), indicating that DNA molecules are randomly, homogeneously orientated and are uncorrelated within the sublayer, consistent with the X-ray analysis.

To show the generality of our approach with regard to other nucleic acids, TLCs from RNA were fabricated following the same complexation procedure (*SI Appendix, Section C*). The resulting TLC phase ranged from −7 to 43 °C (*SI Appendix*, Fig. S6). POM of the RNA–DOAB complex displayed a typical focal-conic texture (Fig. 2*B*), and the analysis of SAXS and WAXS data indicated a smectic mesophase with a layer spacing of 20.3 Å (*SI Appendix*, Fig. S7). The periodic lamellar structures are also directly confirmed by FF-TEM (*SI Appendix*, Fig. S8). Furthermore, it is interesting to note that the DNA or RNA molecules can be liberated from the dehydrated TLCs by exposure to saturated NaCl solution, allowing dissolution in aqueous phase.

TLCs Based on Supercharged Polypeptides and Fusion Proteins. In the next step, TLCs involving polypeptides were investigated. Genetic engineering allows expression of artificial genes in bacterial vectors, encoding polypeptides that represent macromolecules with well-defined sequences, chain lengths, and stereochemistry (35, 36). One such example is elastin-like polypeptides (ELPs), which are based on a common pentameric repeat sequence (VPGVG) found in tropoelastin. Because of the material's inherent mechanical elasticity and inverse temperature-transition behaviors, ELPs have gained considerable attention for biotechnological and biomedical applications (37, 38). Here, we take advantage of the flexibility of amino acid composition in ELPs by introducing glutamic acid at the fourth position of the repeat to transform ELP into unfolded and highly charged anionic polyelectrolytes (38). Thus, genetically encoded ELPs with 72 negative charges along the backbone (E72) and a variant functionalized with green fluorescent protein (GFP) as fusion, E72-GFP, were produced in *Escherichia coli* (*SI Appendix, Section D*).

Both supercharged ELPs formed solvent-free smectic TLCs by using electrostatic interactions between the unfolded peptide chains and the surfactant didodecyldimethylammonium bromide (DDAB) (*SI Appendix, Section D*). Thermal analysis indicated that the ELP–DDAB complexes exhibit liquid crystalline phases from 30 to 80 °C and a water content of 2% (wt) (*SI Appendix*, Figs. S17 and S18). The complexes exhibited birefringent focal-conic textures under POM (Fig. 2*C* and *SI Appendix*, Fig. S16) and, interestingly, showed an isotropic-smectic modulated phase sequence (Fig. 1). At $T = 70$ °C, SAXS profiles of E72–DDAB (Fig. 3*C* and *SI Appendix*, Fig. S21) show a well-defined lamellar diffraction peak at $q = 0.26$ Å^{-1}, as well as its harmonics ($q = 0.521, 0.779$ Å^{-1}). The corresponding layer spacing of $d = 24.4$ Å

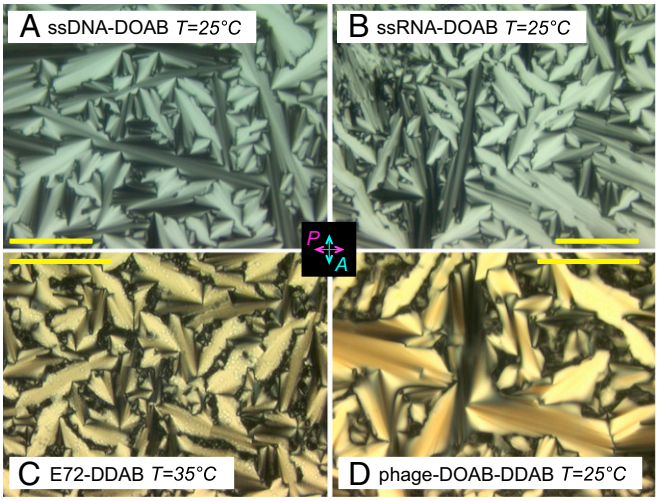

Fig. 2. POM images of the mesophases cooled from isotropic of various biomolecule-surfactant complexes in 10-μm-thick gaps between glass plates. The four images all show planar aligned focal-conic domains having the smectic layers locally normal to the glass. (*A*) 22mer ssDNA–DOAB at 25 °C. (*B*) 22mer ssRNA–DOAB at 25 °C. (*C*) Supercharged ELP E72–DDAB at 35 °C. (*D*) Engineered phage–DOAB–DDAB at 25 °C. (Scale bar, 100 μm.)

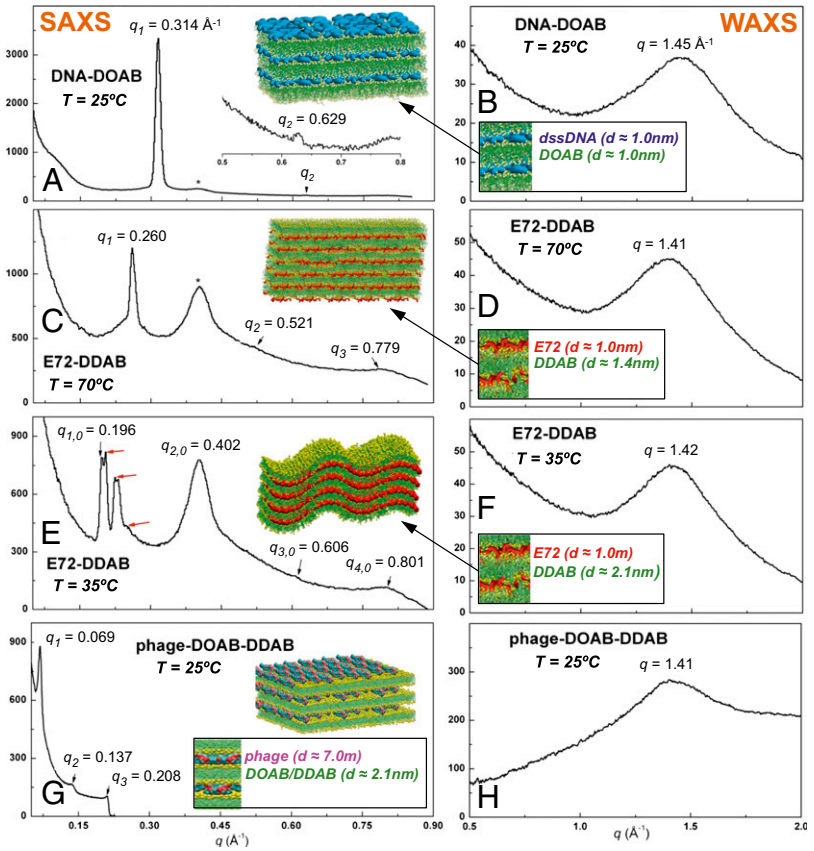

Fig. 3. SAXS and WAXS profiles of the biomolecule–surfactant complexes cooled from isotropic to the smectic mesophases. The corresponding molecular organizations of the different smectic structures (side view) are given in the insets. (*A* and *B*) 22mer ssDNA–DOAB at $T = 25$ °C; the peak at q_2 is magnified in the inset. (*C* and *D*) Supercharged polypeptides E72–DDAB at $T = 70$ °C. (*E* and *F*) E72–DDAB at $T = 35$ °C. The multiple peaks (*red arrows*; $q = 0.196$, 0.205, 0.227, 0.249 Å^{-1}) can be indexed as ($s = 1$, $m = 0$), (*1, 1*), (*1, 2*), (*1, 3*), where s is along the layer normal and m is in the layer plane, indicating an undulated smectic structure of 2D ordering. (*G* and *H*) Engineered phage–DOAB–DDAB at $T = 25$ °C. The diffraction peak at $q \sim 0.4$ Å^{-1} (labeled with * in *A* and *C*) is a result of the kapton, which is used for sample loading and sealing. In *E*, the second-order scattering ($q \sim 0.402$ Å^{-1}) of E72–DDAB is overlapped with that of kapton. The third order scattering ($q_3 = 0.208$) is approaching the limit of the angular range of the distant detector and thus the X-ray intensity drops after this peak.

suggests a bilayer structure with, alternatively, an ELP sublayer ($d \sim 10$ Å) and an interdigitated DDAB sublayer ($d \sim 14.4$ Å) (Fig. 1 and Fig. 3*C*, *inset*). The intralayer packing of the DDAB lipids ($d \sim 4.5$ Å) shows a typical broad peak in the WAXS (Fig. 3*D*). When cooled below $T = 55$ °C in the modulated smectic phase, the layer spacing increases from $d = 24.4$ Å to $d = 31.4$ Å (Fig. 3*E* and *SI Appendix*, Fig. S21), and a set of subsidiary satellite peaks ($q = 0.205$, 0.227, 0.249 Å^{-1}) appears around the smectic layer reflection peak, indexed as (*1, 1*), (*1, 2*), and (*1, 3*) of a 2D rectangular lattice, suggesting an additional periodicity perpendicular to the layer normal; that is, an in-plane layer undulation that, with the layering, forms a type of LC columnar phase. The undulated layer structure is directly visualized by FF-TEM images (Fig. 4 *C* and *D*). The multiple-step "cliffs" show the layer undulation propagating through many layers without changing the smectic structure. This kind of layer undulation has so far been observed in the ripple phase of phospholipids (39) and in the B1 and B7 phases of bent-core LCs (40–42).

This observation indicates that engineered supercharged polypeptides are able to self-assemble into ordered-layer TLC structures in the absence of any solvent, although they did not exhibit a typical α-helical or β-sheet secondary structure. Interestingly, the characteristic fluorescent property of GFP was maintained in the mesophases of the E72-GFP–DDAB complex, indicating that the folded protein was not denatured by the surfactant treatment (*SI Appendix*, Figs. S14, S18, and S22–S24). In contrast, it is noteworthy that the GFP did not disturb the mesophase behavior, although both components exhibit comparable molecular weights. As for the nucleic acids, ELPs (E72 or GFP-E72) can be transferred from the TLC to the aqueous phase by treatment with saturated NaCl solution.

TLCs Based on Virus Particles. Subsequently, we explored whether even much larger, hierarchical biomacromolecular-based superstructures can be manipulated, using the ionic self-assembly approach. For that purpose, engineered M13 bacteriophages were selected, which are monodisperse and anisotropic rod-like particles 1 μm in length and 7 nm in width (9, 10). The virus is enveloped by ∼2,700 copies of the major coat protein pVIII, containing three negatively charged residues close to the N terminus (NH_2-VPGVGAEGDDPA•••-COOH; negatively charged residues are underlined) (*SI Appendix, Section E*). After complexation of the phage with mixed surfactants of DOAB and DDAB (*SI Appendix, Section E*), a smectic mesophase with typical focal-conic birefringence was observed in the range of 14–58 °C (Fig. 2*D* and *SI Appendix*, Figs. S28 and S29). From the SAXS and WAXS measurements (Fig. 3 *G* and *H* and *SI Appendix*, Fig. S30), smectic layer reflection ($q = 0.0686$ Å^{-1}) and its harmonics ($q = 0.1371$, 0.208 Å^{-1}) were observed with a periodicity of 91.5 Å. The layer spacing corresponds to a bilayer structure made of a sublayer of phage (∼70 Å) and an interdigitated sublayer of surfactants (DOAB and DDAB; ∼21.5 Å) (Fig. 3*G*, *inset*). Each repeating layer consists of tail-to-tail interacting surfactants that protrude from the phage particles (Fig. 1). Long-range periodic

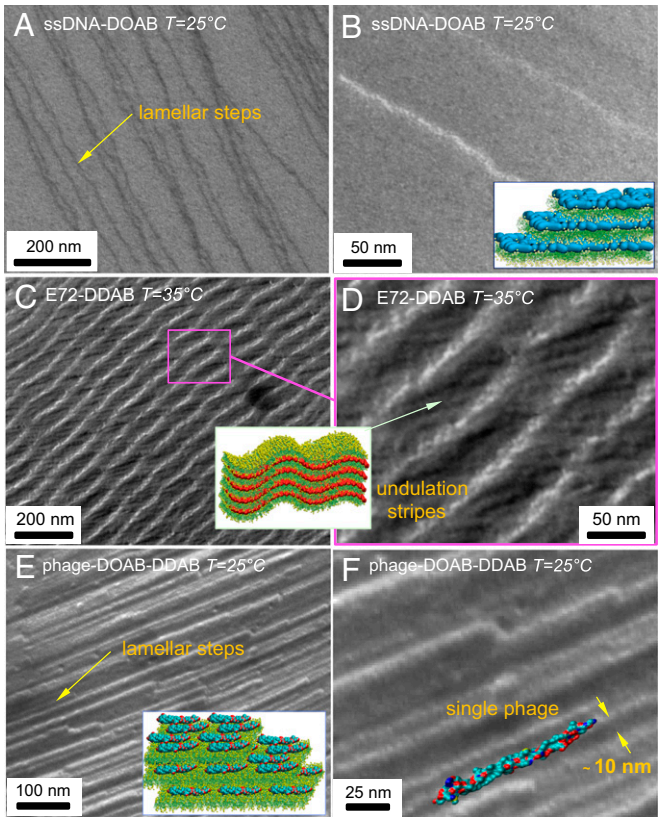

Fig. 4. FF-TEM images of the mesophases formed by the biomolecule–surfactant complexes. The samples were quenched after cooling from isotropic to the desired temperatures in the mesophase, and then fractured in the bulk. The models are sketched in the insets. (*A*) Lamellar structures of the 22mer ssDNA–DOAB with fractured distinct layer steps and, magnified in (*B*), homogeneous layer surfaces with ssDNA molecules randomly oriented within the sublayer. (*C* and *D*) Microstructures of the modulated smectic mesophases observed in the supercharged polypeptide E72–DDAB complexes, showing a 2D periodic lattice: the smectic layers parallel to the image plane and the in-plane layer undulation (*C*, top view; *D*, side view). Periodicities of 17 nm (magenta box), close to the X-ray in-plane modulation wavelength; 12 nm; and 50 nm are evident in the FF-TEM images (*E*) and magnified (*F*). Long-range ordered lamellar structure of the phage–DOAB–DDAB complexes, where individual phage was identified at the layer edges, indicating the orientational order of phages within the sublayer. The layer spacing matches well with the SAXS data.

layer structures in the mesophase have been confirmed by FF-TEM studies (Fig. 4 *E* and *F*). The fractured plane revealed individual phages globally, along a preferred direction. Nematic orientational ordering has developed between different phages within the sublayer as a result of the rigidity and large length-to-diameter aspect ratio of phage (Fig. 1). In contrast to the nucleic acid and protein TLCs, phages cannot be redispersed in the aqueous phase by salt solution treatment because of their fragile structures relying on supramolecular interactions.

Conclusions

We report here a generic molecular architecture and preparative scenario whereby TLCs can be fabricated from biopolymers and large biomacromolecular assemblies with dimensions ranging from only several nanometers up to the micrometer regime. Several important classes of biomaterials including DNA, RNA, polypeptides, fusion proteins, and viruses that exhibit negative charges were complexed with cationic surfactants by a simple fabrication procedure. The biological materials represent a new class of TLCs, which form mesophases that are stabilized by electrostatic interactions. It is important to note that single-stranded short DNA and RNA as well as unfolded supercharged polypeptides assemble into periodic lamellar structures, despite the fact that these molecules lack sufficient rigidity. Genetic engineering is a powerful tool to fabricate de novo designed polypeptide building blocks that are constituent components of TLCs. Moreover, this bioengineering technique allows integration of other functional proteins, which have no LC properties themselves, into TLCs with only little interference with the mesophase. In the future, we will study the properties of the biological components within this novel class of TLCs providing a hydrophobic environment and lacking high dielectric water content. The flexibility of incorporating various different biological building blocks will enable many technological applications including biosensing, biocatalysis, and bioelectronic devices.

Materials and Methods

The detailed procedures for biomolecule production, biosurfactant complex preparation, characterization, and additional data described in this work can be found in the *SI Appendix, Materials and Methods*.

Synthesis of Oligonucleotide and Production of Supercharged Polypeptides and Phage. DNA with the sequence 5′-CCTCGCTCTGCTAATCCTGTTA-3′ was synthesized through the conventional solid-phase synthesis method. Elastin-like polypeptides (E72, E72-GFP) and phage M13 were genetically engineered in *E. coli*.

Preparation of Biosurfactant Complexes. After mixing aqueous solution of oligonucleotide, E72, E72-GFP, or phage with water-soluble cationic surfactants (DOAB or DDAB), precipitate occurred. After centrifugation and lyophilization, biosurfactant complexes were obtained.

ACKNOWLEDGMENTS. The help of Wenqiang Zou in recording the fluorescence spectra is gratefully acknowledged. This research was supported by the European Union [European Research Council Starting Grant and specific targeted research project (STREP): Microscale Chemically Reactive Electronic Agents], the Netherlands Organization for Scientific Research (NWO-Vici, NWO-Echo), the Zernike Institute for Advanced Materials, and the National Science Foundation under Biomolecular Materials Grant 1270606, and Materials Research Science and Engineering Centers Grants DMR-0820579 and DMR-1420736.

1. Nakata M, et al. (2007) End-to-end stacking and liquid crystal condensation of 6 to 20 base pair DNA duplexes. *Science* 318(5854):1276–1279.
2. Koltover I, Salditt T, Rädler JO, Safinya CR (1998) An inverted hexagonal phase of cationic liposome-DNA complexes related to DNA release and delivery. *Science* 281(5373):78–81.
3. Hamley IW (2010) Liquid crystal phase formation by biopolymers. *Soft Matter* 6(9): 1863–1871.
4. Bangham AD (1983) *Liposome letters* (Academic Press, New York).
5. Strzelecka TE, Davidson MW, Rill RL (1988) Multiple liquid crystal phases of DNA at high concentrations. *Nature* 331(6155):457–460.
6. Livolant F (1991) Ordered phases of DNA in vivo and in vitro. *Physica A* 176(1):117–137.
7. Livolant F, Bouligand Y (1986) Liquid crystalline phases given by helical biological polymers (DNA, PBLG and xanthan). Columnar textures. *J Phys* 47(10):1813–1827.
8. Yu SM, et al. (1997) Smectic ordering in solutions and films of a rod-like polymer owing to monodispersity of chain length. *Nature* 389(6647):167–170.
9. Dogic Z, Fraden S (2006) Ordered phases of filamentous viruses. *Curr Opinion in Coll & Inter Sci* 11(1):47–55.
10. Chung WJ, et al. (2011) Biomimetic self-templating supramolecular structures. *Nature* 478(7369):364–368.
11. Ramamoorthy A (2007) *Thermotropic liquid crystals* (Dordrecht, Springer).
12. Briman M, et al. (2004) Dipole relaxation losses in DNA. *Nano Lett* 4(4):733–736.
13. Yamahata C, et al. (2008) Humidity dependence of charge transport through DNA revealed by silicon-based nanotweezers manipulation. *Biophys J* 94(1):63–70.
14. Lewis FD, et al. (1997) Distance-dependent electron transfer in DNA hairpins. *Science* 277(5326):673–676.
15. Hamad-Schifferli K, Schwartz JJ, Santos AT, Zhang S, Jacobson JM (2002) Remote electronic control of DNA hybridization through inductive coupling to an attached metal nanocrystal antenna. *Nature* 415(6868):152–155.
16. Jeffrey GA (1986) Carbohydrate liquid crystals. *Acc Chem Res* 19(6):168–173.
17. Sakya P, Seddon JM (1997) Thermotropic and lyotropic phase behaviour of monoalkyl glycosides. *Liq Cryst* 23(3):409–424.
18. Milkereit G, Vill V (2006) An improved synthetic procedure for the preparation of N-Acyl (2-aminoethyl)-β-d-glycopyranoside lipids and characterization of their mesogenic properties. *J Carbohydr Chem* 25(8-9):615–632.

19. Goodby JW, et al. (2007) Thermotropic liquid crystalline glycolipids. *Chem Soc Rev* 36(12):1971–2032.
20. Perriman AW, Cölfen H, Hughes RW, Barrie CL, Mann S (2009) Solvent-free protein liquids and liquid crystals. *Angew Chem Int Ed Engl* 48(34):6242–6246.
21. Wenzel A, Antonietti M (1997) Superstructures of lipid bilayers by complexation with helical biopolymers. *Adv Mater* 9(6):487–490.
22. Hanski S, et al. (2008) Structural and conformational transformations in self-assembled polypeptide-surfactant complexes. *Macromolecules* 41(3):866–872.
23. Hanski S, Junnila S, Soininen AJ, Ruokolainen J, Ikkala O (2010) Oblique self-assemblies and order-order transitions in polypeptide complexes with PEGylated triple-tail lipids. *Biomacromolecules* 11(12):3440–3447.
24. Tschierske C (2007) Liquid crystal engineering—new complex mesophase structures and their relations to polymer morphologies, nanoscale patterning and crystal engineering. *Chem Soc Rev* 36(12):1930–1970.
25. McBride C, Vega C (2002) A Monte Carlo study of the influence of molecular flexibility on the phase diagram of a fused hard sphere model. *J Chem Phys* 117(22):10370–10379.
26. Faul CFJ, Antonietti M (2003) Ionic self-assembly: Facile synthesis of supramolecular materials. *Adv Mater* 15(9):673–683.
27. Tanaka K, Okahata Y (1996) A DNA-lipid complex in organic media and formation of an aligned cast film. *J Am Chem Soc* 118(44):10679–10683.
28. Okahata Y, et al. (1998) Anisotropic electric conductivity in an aligned DNA cast film. *J Am Chem Soc* 120(24):6165–6166.
29. Neumann T, Gajria S, Bouxsein NF, Jaeger L, Tirrell M (2010) Structural responses of DNA-DDAB films to varying hydration and temperature. *J Am Chem Soc* 132(20): 7025–7037.
30. Gajria S, Neumann T, Tirrell M (2011) Self-assembly and applications of nucleic acid solid-state films. *Wiley Interdiscip Rev Nanomed Nanobiotechnol* 3(5):479–500.
31. Zhou S, Liang D, Burger C, Yeh F, Chu B (2004) Nanostructures of complexes formed by calf thymus DNA interacting with cationic surfactants. *Biomacromolecules* 5(4):1256–1261.
32. Gray GW, Goodby JWG (1984) *Smectic liquid crystals* (Leonard Hill, Glasgow).
33. Zhou J, Gregurick SK, Krueger S, Schwarz FP (2006) Conformational changes in single-strand DNA as a function of temperature by SANS. *Biophys J* 90(2):544–551.
34. Bouxsein NF, et al. (2011) Two-dimensional packing of short DNA with nonpairing overhangs in cationic liposome-DNA complexes: From Onsager nematics to columnar nematics with finite-length columns. *J Am Chem Soc* 133(19):7585–7595.
35. Langer R, Tirrell DA (2004) Designing materials for biology and medicine. *Nature* 428(6982):487–492.
36. Dang JM, Leong KW (2006) Natural polymers for gene delivery and tissue engineering. *Adv Drug Deliv Rev* 58(4):487–499.
37. DiMarco RL, Heilshorn SC (2012) Multifunctional materials through modular protein engineering. *Adv Mater* 24(29):3923–3940.
38. Kolbe A, et al. (2011) De novo design of supercharged, unfolded protein polymers, and their assembly into supramolecular aggregates. *Macromol Rapid Commun* 32(2): 186–190.
39. Sengupta K, Raghunathan VA, Katsaras J (2003) Structure of the ripple phase of phospholipid multibilayers. *Phys Rev E Stat Nonlin Soft Matter Phys* 68(3 Pt 1):031710.
40. Coleman DA, et al. (2003) Polarization-modulated smectic liquid crystal phases. *Science* 301(5637):1204–1211.
41. Coleman DA, et al. (2008) Polarization splay as the origin of modulation in the B1 and B7 smectic phases of bent-core molecules. *Phys Rev E Stat Nonlin Soft Matter Phys* 77(2 Pt 1):021703.
42. Gorecka E, et al. (2008) Modulated general tilt structures in bent-core liquid crystals. *J Mater Chem* 18:3044–3049.